

Combining Rainfall Parameter and Landslide Susceptibility to Forecast Shallow Landslide in Taiwan

C.F. Lee¹, C.M. Huang², T.C. Tsao³, L.W. Wei⁴, W.K. Huang⁵, C.T. Cheng⁶, and C.C. Chi⁷

^{1,2,3,4,5,6} Disaster Prevention Technology Research Center, Sinotech Engineering Consultants, INC, Taipei, Taiwan, (R.O.C.)

² Graduate Institute of Applied Geology, National Central University, Zhongli, Taiwan, (R.O.C.)

⁷ Central Geological Survey, Ministry of Economic Affairs, New Taipei, Taiwan, (R.O.C.)

¹E-mail: cflee@sinotech.org.tw

²E-mail: odin@sinotech.org.tw

³E-mail: tctsao@sinotech.org.tw

⁴E-mail: lwwei@sinotech.org.tw

⁵E-mail: wuangwk@sinotech.org.tw

⁶E-mail: ctcheng@sinotech.org.tw

⁷E-mail: chitc@moeacgs.gov.tw

ABSTRACT: Catastrophic landslides and debris slides triggered by typhoons such as Typhoon Morakot (2009) have occurred more frequently in the recent years, and caused many casualties and much economic loss in Taiwan. For the purpose of reducing the damage and preventing loss of life resulting from geological hazards, this study collects multiple period landslide inventories which contain the information of occurrence time, location, magnitude, rainfall intensity, accumulated rainfall to establish the rainfall threshold for shallow landslides on a regional scale. This study applies the concept of a hazard matrix which combines the magnitude (landslide ratio of slope units) and the possibility of occurrence (historical disaster records) to set up the early warning thresholds. Accordingly, the critical rainfall thresholds are build up based on the R_{24} (24 hours cumulated rainfall) and I_3 (3-hour mean rainfall intensity) of historical records. A validation result shows the model can predict the possible sediment hazard on the hillslope 2~9 hours before occurrence of landslides. The web-GIS based early-warning system is also developed to display the real-time rainfall data and assess the warning signal immediately for disaster prevention through increasing the response time.

KEYWORDS: Shallow landslide, Landslide susceptibility, Slope unit, Rainfall threshold

1. INTRODUCTION

The effect of extreme climate has induced torrential rainfall and landslide disasters world-wide recently. Such a great amount of rainfall usually falls on a specific region rapidly, as a result of which it usually brings severe sediment-related disasters in the mountainous areas. The rainfall thresholds for triggering shallow landslides have been well discussed and determined in the past decade (Chen et al., 2006; Guzzetti et al., 2007; Wu et al., 2011). Different analytical approaches are based on the distinct climate conditions and regional characteristics. The rainfall thresholds related to the sediment hazards can be classified into five categories including intensity-duration (I-D diagram, Brunetti et al., 2010; Zhou et al., 2014), accumulated rainfall-duration (R-D diagram, Martelloni, 2011; Vessia et al., 2014), accumulated rainfall (Corominas and Moya, 1999; Bell and Maud, 2000), intensity-accumulated rainfall, (I-R diagram, Hong et al., 2005) and accumulated rainfall-accumulated rainfall (R-R diagram, Osanai et al., 2010; Turkington et al., 2014). Generally, neither the magnitude nor the types of landslide are taken into consideration for rainfall threshold analysis, so the regional rainfall thresholds obtained from the above approaches may overestimate or underestimate. It is obvious that the occurrence of shallow landslides depends more on the rainfall intensity, accumulated rainfall, and degree of weathering (hillslope) in comparison with deep-seated landslides. Most historical typhoon events in Taiwan also prove clearly that the spatial distribution of regional shallow landslides is located in areas with high rainfall concentration. Additionally, the early warning rainfall threshold for potential debris flow torrents in Taiwan has been established and applied to evacuation planning for decades. The total number of the potential debris flow torrents has increased quickly and is currently 1673. On the basis of long-term hazard analysis, the critical rainfall threshold for triggering debris flow has been established for each potential torrent. However, the rainfall threshold for shallow landslides on a national scale in Taiwan is still incomplete and in need of development. Recent studies related to landslide hazards have been focusing on watershed scale or specific

local sites using different analysis methods (Chang et al., 2008; Chang and Chiang, 2009; Keijsers et al., 2011). For the purpose of planning operating procedures and disaster prevention, a national scale critical rainfall index which covers slopelands of urban and mountainous areas at risk for shallow landslides is needed for systematic evaluation.

This study presents an innovative approach to combine the magnitude of landslide and rainfall thresholds derived from the Central Weather Bureau (CWB), Taiwan. Adopting the concept of the hazard matrix, the work establishes the rainfall thresholds for slope units in the whole Taiwan area. This work also explores the relationship between the landslide and rainfall characteristics and found that 3 hours mean rainfall intensity and 24 hours accumulated rainfall are the most dominant parameters. The approach was later verified by landslides triggered by typhoons during 2014. Regardless of any further application, a real-time rainfall data set (Quantitative Precipitation Estimation and Segregation Using Multiple Sensor, QPESUMS) which updated hourly has been introduced to construct a Rainfall-induced Landslide Early Warning System (RiLEWS). This system can complement the inadequate warning information for a regional landslide disaster while a rainstorm is approaching. Several applications associated with disaster mitigation may develop for different aspects and protected objects (*i.e.* villages, road sections close to slopeland, and sediment volume in source areas on potential debris flow torrents).

2. STUDY AREA

Taiwan is located in the western Pacific Ocean, at the convergent plate boundary zone of Philippine Sea plate and Eurasian plate, causing hundreds of faults and folds in the 35,833 km² area because of tectonic activity (Figure 1). The major geological units of the island of Taiwan can be separated into the Coastal Plain (CP), Western Foothills (WF), Hsueshan Range (HSR), West Central Range (WCR), East Central Range or Tananao Schist complex (ECR), Longitudinal Valley (LV), and Coastal Range (CR) from the western to the eastern coast (Central Geological Survey, Taiwan).

Typhoons and monsoons bring large amounts of rainfall which is estimated at from 2,500 mm to more than 3,000 mm in mountainous areas annually (Hsu et al., 2013). As a result, the exhumation rate in Taiwan is about 3 to 6 mm/year (Dadson et al., 2003), and is mainly caused by the the landslide process. On the other hand, the high population density (647 population/km²) and the frequent natural disasters mean that Taiwan is one of the most dangerous countries and is exposed to multiple hazards (Dilley et al., 2005). This study divided Taiwan into four main regions including the northern, central, southern, and eastern Taiwan (Figure 1). These areas are the most populated and are faced with the threat of shallow landslides.

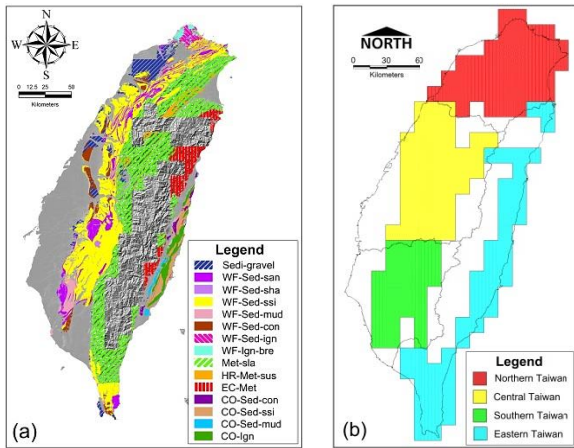


Figure 1 (a) Geological settings and (b) study area in the work

(geologic legend: Sedi: sedimentary rock; WF: western foothills; Met: metamorphic rock; HR: Hsuehshan range; EC: Eastern flank of central range; CO: Coastal range; san: sandstone; sha: shale; ssi: sandstone-shale interbedded; nud: mudstone; con: conglomerate; ign: igneous rock; bre: breccia; sla: slate; sus: submetamorphism sandstone)

3. METHODOLOGY

This study aims to establish the rainfall thresholds for the debris slide, thus, the landslide must be interpreted first to build up the landslide inventory. After building up the inventory, field investigation is needed to check the results of the interpretation, the mechanism and the geological conditions of each landslide. The occurrence time of landslides is crucial information with respect to establishing the rainfall thresholds; therefore, this research also includes visits with the village chief and the resident around the landslide to record this information. With this information, accumulated rainfall and the rainfall intensity can be calculated. Combining the results of landslide susceptibility and the historical landslide cases which containing the rainfall conditions, the rainfall thresholds can be established and an early-warning system can also be built to reduce the loss of life and property.

3.1 Mapping of Landslide Inventory and Field Investigation

Landslide mapping can be conducted through the interpretation of remote sensing images such as aerial photos, satellite images, and digital elevation models. The texture, shape, shades, and topographical characteristics are used to define the landslide feature and boundary (Asselenand et al., 2006; Moine et al., 2009; Mondini et al., 2011; Stumpf and Kerle, 2011; Martha et al., 2012; Razak et al., 2013). This work uses satellite image (SPOT-5) for the interpretation of landslides induced by several typhoon events. Field investigation has been carried out for the validation of interpretation and mapping (Figure 2). Detailed information including mechanism, lithology, geologic structure, joint, strength of rocks, and sliding depth were also recorded for further analysis. The landslide

inventories obtained from different specific events also provide a preferable input for landslide susceptibility analysis.

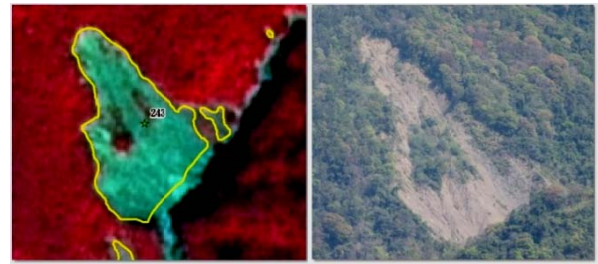


Figure 2 Landslide interpretation and the picture taken during the field investigation for the validation

The rainfall conditions that induced landslides are important data while applying the empirical method to establish the rainfall thresholds for debris slide (Guzzetti et al., 2007, 2008; Brunetti et al., 2010). A total of 941 landslide cases which contained information regarding occurrence time were collected during the field investigation (Figure 3). In addition, for the purpose of conserving these valuable records and providing for further analysis, a landslide disasters database was established. This database consists of four parts: (1) basic data (location, occurrence time, typhoon event, area, geological condition, geomorphological conditions); (2) map which shows the location of landslide; (3) photos of the field investigation which highlight some important features; (4) reconnaissance report of the landslide. The database provides a systematic method for collecting data on wide-spread landslide cases.

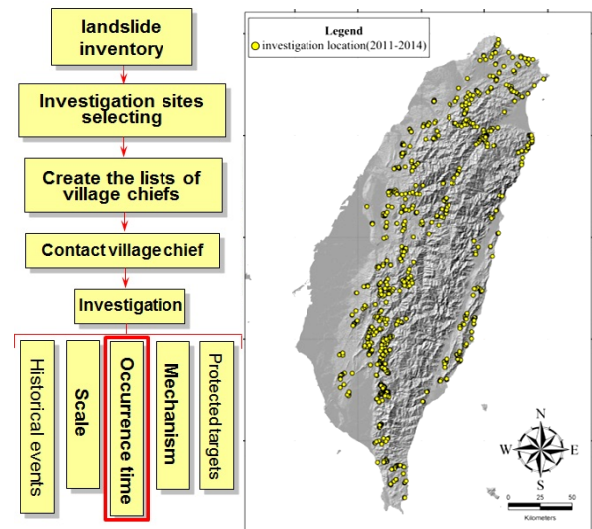


Figure 3 Flowchart of recording the occurrence time of landslide during field investigation

3.2 Rainfall Data Collection

On the basis of the occurrence time for each landslide event, the rainfall data was collected and analyzed to understand the rainfall conditions. In Taiwan, both high intensity and long duration rainfall events cause severe disasters frequently (Chen et al., 2006; Wu et al., 2011). As mentioned above, this work collected more than 941 landslide (debris sliding) events in Taiwan from 2011 to 2014. The preliminary rainfall analysis for occurrence time stated that 48.9% of the events happened within 1.5 hours of peak rainfall intensity (Table 1). It also shows that approximately 50% of debris sliding was triggered by maximum rainfall intensity or after 3 hr of peak rainfall intensity occurring over a short time. In comparison with landslide events induced by high rainfall intensity, 51.1% of

hillslope sliding is dominated for long-term cumulative rainfall. Hence, this study chooses 3-hour mean rainfall intensity (I_3) as the short-term rainfall index and 24-hour accumulated rainfall (R_{24}) as the long-term rainfall indices (Liao et al., 2010). Figure 4 shows the method for calculating the rainfall indexes. The segment principle of rainfall event is defined as the rule of 4 mm (beginning) - 6 hr (duration) - 4 mm (ending). This means the rainfall starts to be calculated when the cumulative rainfall is greater than 4 mm. Once the hourly rainfall is lower than 4 mm for 6 sequential hours, and then the total cumulative rainfall value ends. For the purpose of understanding the rainfall spatial distribution on regional scale, inverse square distance weighting (IDW) method was chosen for wide-area interpolation method of rainfall analysis, and providing rainfall input parameters in landslide susceptibility analysis in Sec. 3.5. IDW method suggests that the observed and estimated data obey a linear relationship. The magnitude of weighting factors is inversely proportional to the square of distance between the observed and estimated points. The rainfall data (\bar{P}) for each landslide at specific slope unit at any time can be obtained as follows,

$$\bar{P} = \sum_{i=1}^n w_i P_i, w_i = \frac{h_i^{-2}}{\sum_{i=1}^n h_i^{-2}} \quad (1)$$

where, \bar{P} is the rainfall estimation of observed point (unit: mm); P_i represents the real rainfall value in observed point (unit: mm); w_i and h_i are the weighting factor and horizontal distance between landslide location and rainfall gauge station; n depicts the number of rainfall gauge stations adopted in above analysis.

Table 1 rainfall analysis area for occurrence time of shallow landslide events in Taiwan

| occurrence time of landslide | number | percentage |
|---|--------|------------|
| within 3 hr of rainfall peak intensity (triggering by rainfall intensity) | 218 | 23.2% |
| within 3 hr of 2 nd or 3 rd highest rainfall intensity (triggering by rainfall intensity) | 242 | 25.7% |
| does not occur on the peak rainfall intensity (triggering by cumulative rainfall) | 481 | 51.1% |
| total | 941 | 100% |

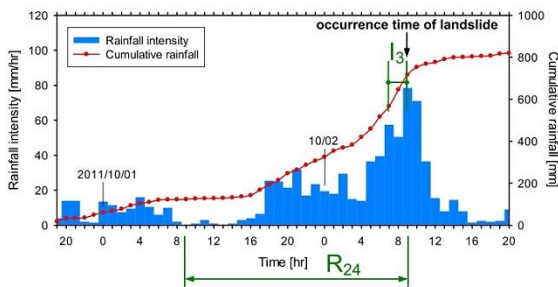


Figure 4 Rainfall indices used in the study

3.3 Generation of Slope Unit

Landslide susceptibility (Lee et al., 2004, 2008^a, 2008^b) described in this study is generated using slope unit (SU) as the analysis element. Slope unit is a slope surface area combining with similar topographical features and geological characteristics (Guzzetti et al., 1999; Xie et al., 2004; Figure 5). The boundaries of slope units were segmented mainly with river valleys and mountain ridges which fit the terrains and topography. All the factors on slope units will be averaged to obtain a representative value when comparing with grid cell approach. The slope unit is a helpful tool in natural hazard management, and it can establish a clear decision making system for pre-disaster landslide mitigation management or post-disaster operations for government agencies. Once the landslide

management database is established, it can assist government agencies in conducting early warning and decision-making for hillslope hazards.

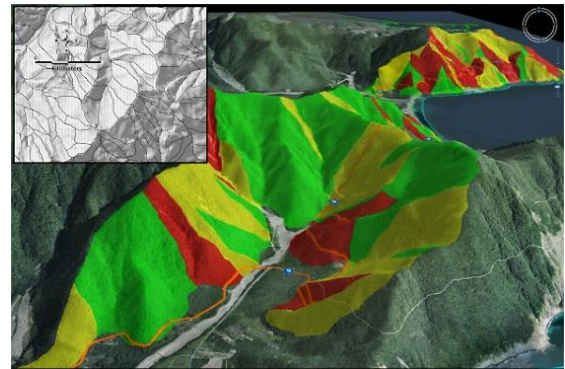


Figure 5 three-dimensional view of slope unit (inset: plane view). The different color of each slope unit represents distinct landslide susceptibility

3.4 Landslide susceptibility analysis (LSA)

Landslides, in which the failing mass is primarily comprised of debris and earth such as weathered bedrock, colluvium or loose, fractured bedrock and failures are via sliding or falling, are referred to as debris slides. The mobilization over gentle slopes is generally via sliding and on steep slopes via falling. Debris slides generally occur on steep slopes and are often triggered by rainfall or intense earthquakes. After the failure, a long and narrow strip of exposed earth, or scar, is left behind. Loose debris on the scar often deposits at the toe of the landslide. This type of debris slide continues to enlarge as a result of prolonged movement and severe scour readily occurs in areas lacking vegetative cover. Clearly, such landslide mechanisms are related to the lithology, topography, and overall geologic structure of the slope. Additionally, external effects such as precipitation and earthquakes also affect the landslide. This study uses a 10 m x 10 m gridded digital terrain model, 1/25,000 bedrock engineering geology map, and environmental geology map in combination with geographic information system software (*i.e.* Eradas Imagine, ArcGIS and MapInfo) paired with Fortran programming developed for this study to estimate the unit slope factor of each unit slope (Figure 6). Once factor selection is completed, graph interpretation and correlation analysis are used to perform a comprehensive evaluation of the factor. Using this analytical approach, the influence of each factor on landslide processes is assessed. These results are then referenced to identify the factors that have the most influence on landslide processes based on geological zoning.

The logistic regression method is applied in this study to evaluate the susceptibility of each slope unit (Guzzetti et al., 1999; Ayalew and Yamagishi, 2005). The landslide susceptibility factors which are selected in the model include material property (classification of rock strength), topographical characteristics (dip slope, height of slope, slope roughness, mean gradient, mean elevation, ratio of steep slope, terrain curvatures, and terrain roughness), geological structure (fault density and fold density), and rainfall parameters (mean 3-hourly intensity and cumulative 24-hr rainfall; shown as in Table 2, (Franklin, 1975; Wilson and Gallant, 2000). So far as factor determination is concerned, both gradient and terrain roughness are most influential factor on landslide susceptibility analysis in this study. Gradient used in the work was extracted from 3x3 mesh grid to calculate the slope at the center of the cell (cell size: 10 m; Wilson and Gallant, 2000). Terrain roughness, which indicates the standard deviation of terrain height by means of calculating 13x13 matrix, is also an important hydrological index to describe landslide characteristic (Kirkby, 1975; Wilson and Gallant, 2000; Lee, 2014).

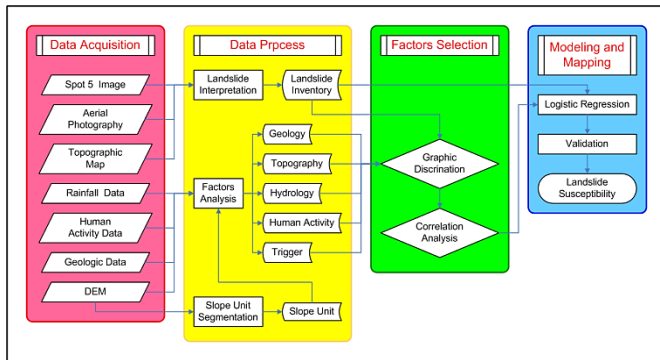


Figure 6 The flowchart of the landslide susceptibility model (revised from Cheng et al., 2013)

The logistic regression method is a special form of log-linear model, specifically when the dependent variable is a binary variable. The formula is described as follows:

$$\ln\left(\frac{P_i}{1-P_i}\right) = \alpha + \sum_{k=1}^k \beta_k x_{ki} \quad (2)$$

where, P_i is the landslide susceptibility index (LSI) at the i^{th} slope while k landslide susceptibility factors ($x_{1i}, x_{2i}, \dots, x_{ki}$) are given. In LSA, x_{ki} is the landslide susceptibility factor of the i^{th} slope, such as slope gradient, slope height, and rock characteristics, etc. If the i^{th} slope is taken as the landslide sample, then $P_i=1$, and non-landslide sample is $P_i=0$. Through logistic regression analysis, coefficient β_k for landslide susceptibility factors and regression constant α can be obtained for the i^{th} slope. By inputting a given landslide susceptibility factor value x_{ki} of any slope into the model, the landslide susceptibility of that slope can be obtained.

Table 2 Factor selection for four analysis areas

| Factor | N | C | S | E |
|---|---|---|---|---|
| classification of rock strength (I, II, III, IV, V) | ○ | ○ | ○ | ○ |
| dip slope | ○ | ○ | ○ | ○ |
| gradient | ○ | ○ | ○ | ○ |
| slope roughness | ○ | ○ | ○ | ○ |
| ratio of steep slope | ○ | | ○ | ○ |
| height of slope | | ○ | | |
| elevation | ○ | | | |
| terrain curvatures | | ○ | ○ | ○ |
| terrain roughness | ○ | ○ | ○ | ○ |
| fault density | ○ | ○ | | |
| fold density | ○ | ○ | ○ | ○ |
| moisture index | ○ | ○ | ○ | |
| 3-hour mean intensity | ○ | ○ | ○ | ○ |
| 24-hr cumulative rainfall | ○ | ○ | ○ | ○ |

¹N, C, S, and E indicate the analysis area in northern, central, southern, and eastern region in Taiwan.

Previous landslide susceptibility studies have considered geologic zoning as the basis of the study and accordingly selected factors to assess landslide susceptibility. However, there may be many unit slopes within a single geologic zone. If a geologic zone is divided into a small number of unit slopes, a model that predicts landslide potential based on those unit slopes may not be representative or significant. To account for this phenomenon, this study appropriately edits the unit slope boundaries in a gradual sloped geologic zone comprised of a low-slope hill, a river terrace that also includes protected targets that would be at risk if a natural disaster were to occur. Additionally, in order to limit the number of zones and take account of patterns in precipitation, the boundaries of the geologic zones used in this study run along watershed

boundaries and divide Taiwan into four zones (Figure 1): northern, central, southern, and eastern regions. This study defines a slope unit as a landslide-slope unit if landslide units account for at least 1% of the slope units or landslide area greater than 400 m². Any slope unit that do not meet this criterion are categorized as a stable-slope unit. The landslide inventory acquired from Sec. 3.1 is incorporated into this study. Landslide samples from the inventory are divided equally into two data sets based on a random sorting process: data set 1, which is used as training data, and data set 2, which is adopted for model validation. As a final step, the models which are developed to estimate landslide potential are examined with error matrix, success rate curve (SRC) or prediction rate curve (PRC) to evaluate the reliability of landslide prediction results. The landslide susceptibility model is highly relates to the effect of regional landslide histories, so the landslide susceptibility should be updated when new landslide event were available in the region. The reasonable update period on regional scale is approximately 4~5 years to avoid false alarms on reactive landslide area.

3.5 I₃-R₂₄ diagram model

This study uses the “landslide ratio of the slope unit” to categorize landslide disaster severity. Using the landslide characteristics and the landslide ratio of the slope unit, the landslide severity is classified as: Type I - high landslide ratio, Type II - moderate landslide ratio and Type III - low landslide ratio. The equation for estimating the landslide ratio of the slope unit is described below:

$$\text{landslide ratio (\%)} = (A_{LS} / A_t) * 100\% \quad (3)$$

where, A_{LS} : landslide area in the slope unit; A_t : total area of the slope unit. Landslide-slope units are categorized according to landslide disaster severity through Eq.(3). Regarding a stable-slope unit, because landslide records are not available for the unit slope, the severity cannot be assessed by adopting the approach applied to landslide-slope units. Therefore, an attempt was made to develop a relationship between landslide ratio and susceptibility using available observation data. This method was applied to the four Taiwan geologic zones. Each landslide location was distinguished using a landslide susceptibility value of 0.05. Using only the landslide ratio values in slope units within two standard deviations of all the values that occurred within each zone, the largest landslide ratio possible was identified. Combining the relationship, the landslide susceptibility associated with an undisturbed unit can be assessed based on the disaster severity.

After analyzing more than 900 cases, 3-hour mean rainfall intensity and 24-hour cumulated rainfall were chosen as the index for establishing rainfall thresholds for debris slide. Historical records of landslides are plotted in Figure 7, and the formula for ellipse is adopted to determine the envelope curve of historical cases. The parameter a and b of the ellipse are set according to the slope of regression line by applying the least square method. The thresholds are determined according to the percentage of historical cases that are included by the envelope curve, e.g. the 90% threshold includes 90% of the historical landslide cases. It means that if the rainfall condition exceeds this threshold, the probability of occurring landslides is extremely high. Additionally, this study considers disaster severity and landslide ratio in the form of a hazard matrix to develop landslide warning levels. As shown in Figure 8, Type I landslide severity has a high landslide ratio and large scope of influence. Resultantly, once the probability of occurrence exceeds 60%, a red warning level (high danger) is issued. If the probability of occurrence is between 30% and 60%, an orange level warning is issued (moderate danger). And if the probability of occurrence is less than 30%, a yellow warning is issued (low danger). Under typical conditions, such as periods of no rainfall, a green warning is issued (normal conditions). Type II landslide severity has a lower landslide ratio and influence scope relative to Type I. Resultantly, only after a probability of occurrence of 90% or greater is obtained, would a red warning be issued. For a probability of occurrence

between 60% and 90%, an orange warning is issued and between 30% and 60%, a yellow warning is issued. Below 30% or under no rainfall conditions, a green warning is issued. Type III landslide severity is associated with slope units that have the lowest landslide ratio and smallest influence scope. This type of landslide may only include the small slides adjacent to a highway or small magnitude geologic hazard. With respect to the warning signal of the hazard matrix, only after the probability of occurrence exceeds 90%, is an orange warning issued. Between 60% and 90% a yellow warning is issued and below 60%, a green level is issued.

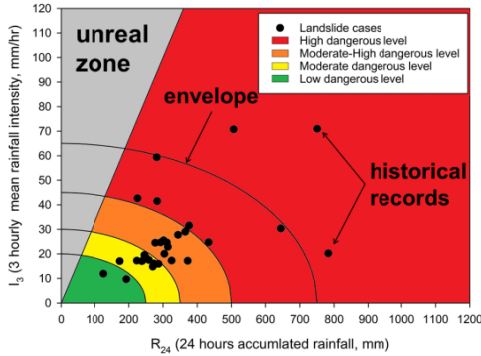


Figure 7 Establishing rainfall thresholds by adopting I_3 and R_{24} as indices to evaluate the probability of landslides occurring under different rainfall conditions

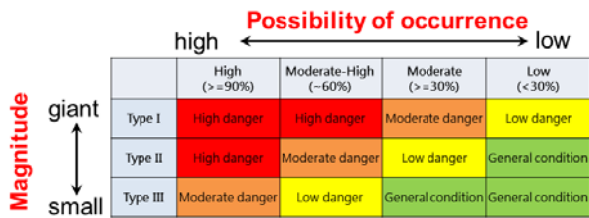


Figure 8 Setting of warning signals combining the magnitude, the possibility of occurrence and the hazard matrix concept

4 RESULTS AND VALIDATIONS

4.1 Rainfall statistics for triggering shallow landslides

In this work, Taiwan was divided into four main regions (Fig. 1) and the preliminary rainfall threshold for each magnitude in each distinct region was established (Figure 8). These thresholds also reflect the complexity and the difference in geology and rainfall characteristics in each area. For example, northern Taiwan consists mainly of volcanic and metamorphic rocks while southern Taiwan is mainly sedimentary and metamorphic rocks, but the MAP (mean annual precipitation) is higher in southern Taiwan. Hence, the rainfall threshold in northern Taiwan shows a slightly higher value to induce a new landslide in comparison with southern Taiwan. So as to clarify the influence of geologic zoning, the study compared the rainfall characteristics for triggering shallow landslide events (Figure 9). The statistical results pointed out the variation among accumulated rainfall (R), mean intensity (I_{mean}), and duration (D) of shallow landslide in three major geologic zones from 941 cases is not significant. The average rainfall index as R , I_{mean} , and D of the landslides are 348 mm, 14.1 mm/hr, and 22.5 hr, respectively. The locations of shallow landslide are almost all concentrated in metamorphic ($n=484$) and sedimentary ($n=415$) zones because the area of plutonic zone ($n=42$) in Taiwan is much smaller than the above mentioned zones. This is the reason Taiwan was divided into to four main zones to study the rainfall characteristic instead of using geological zonation. Some literature also reports and confirms that shallow landslides are actually dependent on the rainfall amount and intensity, and that deep-seated landslides may be determined by

local geological structure and ground water response (Zêzere et al., 2005; Prokesova et al., 2012; Padilla et al., 2014).

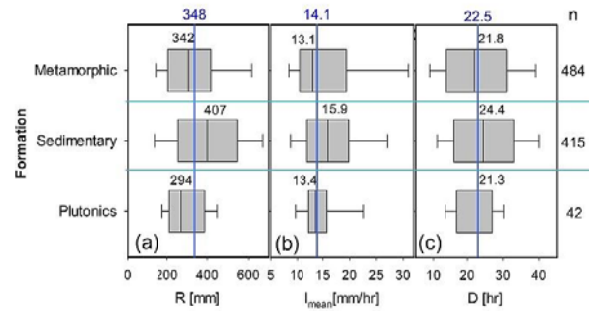


Figure 9 Rainfall statistics analysis from 949 shallow landslide events in different formations. (a) total cumulated rainfall; (b) mean rainfall intensity; (c) rainfall duration for triggering shallow landslides (n is the landslide events collected for analysis)

Ten important typhoon events which caused wide-area shallow landslides were selected to explore the rainfall characteristics (R , I_{mean} , D , R_{24hr} , and I_{3hr}). As shown in Figure 10, 706 cases were taken into analysis in total. From these data it can be observed that an obvious difference is enhanced by typhoon disasters based on the track and intensity. Generally speaking, the averaged trends of cumulated rainfall, mean rainfall intensity, and duration for such critical typhoon events are similar to the results in Figure 9. However, these typhoon events show a slightly higher value that emphasizes the danger level of widespread sediment-related disasters when compared to other rainfall scenarios. Figures 10 (d)-(e) also illustrates the discrepancy between the model parameter (R_{24hr} , I_{3hr}) and the usual rainfall index (R , I_{mean} , and D) on the rainfall index for inducing shallow landslides. It seems to imply that a greater short-term rainfall index ($I_{3hr}>28.8$ mm/hr; Figure 10 (e)) can more easily trigger trigger extensive landslides than long-term cumulative rainfall (R_{24hr}). These results are consistent with field investigations and previous studies. Regarding the typhoon track, the study found the type of typhoon scenario which crosses Taiwan from the eastern coastal range to the western foothills (track No.1, 2, 3, and 4 defined by CWB) may bring a great amount of total rainfall and extend the influenced area.

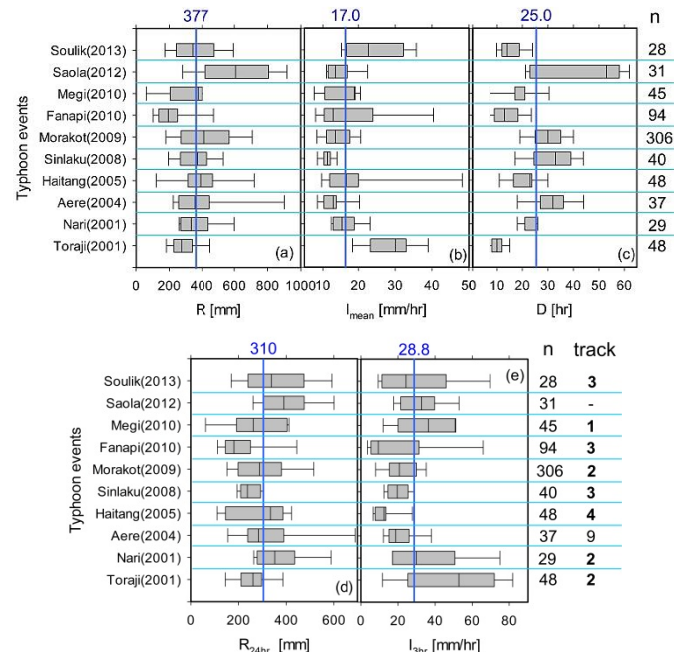


Figure 10 The relationship among the total rainfall, mean rainfall characteristics for ten typhoon events which caused extensive landslide disaster

The rainfall data of nineteen deep-seated landslide disasters caused by typhoon Morakot (2009) in southern Taiwan were analyzed to interpret the landslide type (Figure 11). The intensity-cumulated rainfall threshold can aid in the clarification of shallow and deep-seated landslides (otherwise referred to as large-scale rock slide). However, the mean rainfall intensity (I ~18-58 mm/hr) for both types of landslides is overlapped and it is difficult to distinguish the characteristic. For these cases, large-scale landslide evaluation usually needs to take into account the response of ground water beneath the geologic stratum, so the total cumulated rainfall seems to be an appropriate rainfall index to determine the threshold for triggering a deep-seated landslide ($R > 890$ mm).

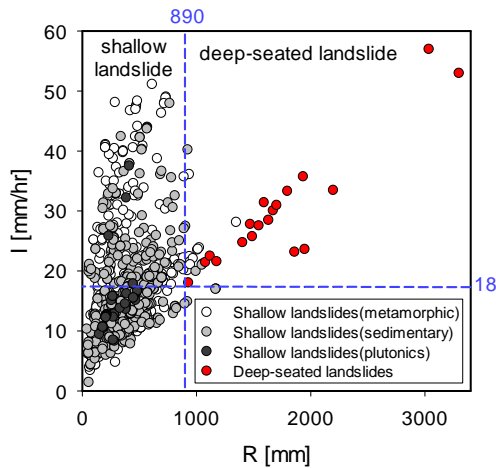


Figure 11 the relationship between total rainfall and mean rainfall intensity for 941 shallow landslides and 19 deep-seated landslides

4.2 Results of landslide susceptibility analysis

Accuracy and success rate curves can be used to differentiate the validity of the landslide susceptibility model. This study defines a susceptibility value of 0.5 to categorize all slope units as being landslide or non-landslide. From this definition, the model accuracy is assessed. Landslide susceptibility value and the classification based on the landslide inventory are compared and used to evaluate the success rate. The calculation approach associated with the accuracy can be expressed using the error matrix. The corresponding equations are listed below:

$$\text{landslide group accuracy} = N_1 / (N_1 + N_2) \quad (4)$$

$$\text{non-landslide group accuracy} = N_4 / (N_3 + N_4) \quad (5)$$

$$\text{overall accuracy} = (N_1 + N_4) / (N_1 + N_2 + N_3 + N_4) \quad (6)$$

where, N_1 is the total number of slope units classified as landslide slope units using the landslide susceptibility analysis that are actually landslide slope units listed in the landslide catalog. N_2 is the total number of slope units classified as non-landslide slope units using the landslide susceptibility analysis that are actually landslide slope units listed in the landslide inventory. N_3 is the total number of slope units classified as landslide slope units using the landslide susceptibility analysis that are actually non-landslide slope units in landslide inventory. N_4 is the total number of slope units classified as non-landslide slope units that are also listed as non-landslide slope units in the landslide inventory. The accuracy of the landslide group is represented by the ratio of the number of landslide-slope units classified by the model to the total number of landslides listed in the inventory. The non-landslide group accuracy is, likewise, the ratio of the number of non-landslide slope units classified by the model relative to the total number of non-landslide slope units listed in the inventory. The quotient of the number of slope units that were

correctly classified as landslide and non-landslide and the total number of slope units is the overall accuracy.

Since disaster prevention efforts are responsive in nature, this study primarily uses the landslide group accuracy to assess the accuracy of the model. The overall accuracy of the model considers the degree of incorrect classifications and provides an accuracy measurement representative of landslide and non-landslide prediction results. The success rate curve and prediction curve is used to assess the ability of the model to interpret training and prediction data (Table 3). Utilizing the Area Under Curve (AUC), the performance of the model is assessed. For AUC values between 0 and 1, when the AUC value is near 1, a smaller range is required to interpret landslide area. Conversely, when the AUC value is near 0, a large range of values is needed to interpret the landslide area. In general, the larger the AUC value, the better the model. The results of the model are not representative when the AUC is lower than 0.5.

This study divided Taiwan into four zones. For each zone, landslide events that were triggered during events that caused expansive landsliding across the zone are adopted as the sample group. For the northern zone, events that caused extensive landsliding were Typhoons Nari, Aere, and Talim and are used to run model training. Utilizing the landslides from these storms, validation results show a cumulative landslide and stability accuracy of 80% (AUC=0.854, Table 4). This result demonstrates that the model is very steady and reliable. The central and southern zones use the Typhoons Sepat and Sinlaku as the training data. The modeled landslide and non-landslide cumulative accuracy is 64% (AUC=0.729) and 61% (AUC=0.608), respectively. The eastern coast model uses landslides associated with Typhoons Haitang, Sepat, Morakot, and Namadol. Results show that the modeled landslide and non-landslide cumulative accuracy is 75% (AUC=0.718). Overall, the performance of the model for each zone is reasonable and demonstrates that the model can be applied to predict landslide activity for non-extreme typhoons or other precipitation events. Additionally, since precipitation associated with rainfall is heavily affected by the path of the typhoon, variations in the distribution of the rainfall have an important effect on the predictive ability of the model. In order to improve the predictive ability of the model for future typhoon events, the current database need to be updated with all new rainfall-triggered landslide data.

Table 3 Training accuracy and AUC of the model in each zone

| Analysis area | ALS | ANLS | TA | AUC |
|-----------------|--------|--------|--------|-------|
| Northern Taiwan | 80.81% | 80.73% | 80.73% | 0.862 |
| Central Taiwan | 75.57% | 70.09% | 71.31% | 0.777 |
| Southern Taiwan | 73.24% | 70.86% | 70.98% | 0.767 |
| Eastern Taiwan | 81.70% | 75.34% | 75.69% | 0.836 |

ALS: Accuracy of landslide set; ANLS: Accuracy of non-landslide set; TA: Total Accuracy

Table 4 Verification accuracy and AUC of the model in each zone

| Analysis area | ALS | ANLS | TA | AUC |
|-----------------|--------|--------|--------|-------|
| Northern Taiwan | 82.18% | 79.58% | 79.73% | 0.854 |
| Central Taiwan | 63.67% | 64.55% | 63.76% | 0.729 |
| Southern Taiwan | 68.08% | 61.57% | 61.47% | 0.608 |
| Eastern Taiwan | 68.11% | 75.78% | 75.11% | 0.718 |

ALS: Accuracy of landslide set; ANLS: Accuracy of non-landslide set; TA: Total Accuracy

4.3 Rainfall threshold for shallow landslide

Utilizing the methods described in Section 3.5, landslide disaster severity analysis results are listed in Table 5. For landslide susceptibility values greater than 0.844, landslide disasters are more likely to occur on slope units having a landslide ratio greater than 0.25 relative to other slope units. These slope units are categorized as "Type I, high landslide ratio" slope units. If the landslide

susceptibility value is equal to or less than 0.515, the landslide disasters resulting from slopes having a landslide ratio of 0.10 or less are the most likely. These slope units are categorized as “Type III, low landslide ratio” unit slopes. If the landslide susceptibility value associated with the slope unit is between 0.515 and 0.844, the slope unit is categorized as a “Type II, moderate landslide ratio” slope unit. The rainfall threshold required to trigger landslide activity is calibrated based on this slope unit categorization system.

Table 5 Landslide susceptibility and magnitude classification in central Taiwan

| landslide ratio | landslide susceptibility | landslide magnitude |
|-----------------|--------------------------|---------------------------|
| 0.30 | 0.910 | 0.844 ~ 1.000 Type I |
| 0.25 | 0.844 | |
| 0.20 | 0.764 | 0.515 ~ 0.844 Type II |
| 0.15 | 0.661 | |
| 0.10 | 0.515 | 0.000 ~ 0.515 Type III |
| 0.05 | 0.265 | |

As mentioned, this study divides Taiwan into four zones: northern, central, southern and eastern. For each zone, a landslide triggering rainfall threshold is constructed. As a result of site specific characteristics including geology, topography and rainfall, the landslide triggering rainfall threshold associated with each landslide disaster severity varies by location (Figure 12). In the northern zone, most landslide hazards are categorized as having a moderate landslide ratio, but in the southern zone, most landslide hazards are categorized as having a low landslide ratio (Figures 12 (a)-(c)). Resultantly, Type I slope units are generally slope units having a landslide ratio greater than 12%. The Type II slope units are generally unit slopes having a landslide ratio that varies between 9% and 12%. The Type III slope units have a landslide ratio of less than 9%. The calibrated rainfall thresholds for each type of slope unit are listed in Table 6. If 24-hour accumulated rainfall is between 500 to 550 mm or the 3-hour mean rainfall intensity is greater than 50mm/hr, a red warning is issued (high dangerous level). If 24-hour accumulated rainfall exceeds 300 to 450 mm or the 3-hour mean rainfall intensity is between 30 to 45 mm/hr, an orange warning is issued (moderate-high dangerous level). If 24-hour accumulated rainfall is between 200 to 300 mm or 3-hour mean rainfall intensity is between 20 to 30 mm, a yellow warning is issued (moderate dangerous level). Any precipitation amounts that are less than those thresholds represent a green warning level (low danger level). Regarding shallow landslide hazards in central Taiwan (Figures 12(d)-(f)), slope units that are categorized as Type I are all slope units having a landslide ratio greater than 25%. Type II slope units are slope units having a landslide ratio between 10% and 25%. Additionally, the slope units with landslide ratio less than 10% are categorized as Type III. The rainfall thresholds for each type are listed in Table 7. Rainfall thresholds corresponding to landslide danger levels in the southern and eastern zones in Taiwan are shown in Figs. 12(g)-(l), and Tables 8, 9. In general, rainfall thresholds are slightly higher in the southern zone relative to the northern, central and eastern zones. Current research results can already be applied as a reference for establishing preliminary warning systems. However, long term validation of these values against future precipitation events and sequential update of the values is still needed.

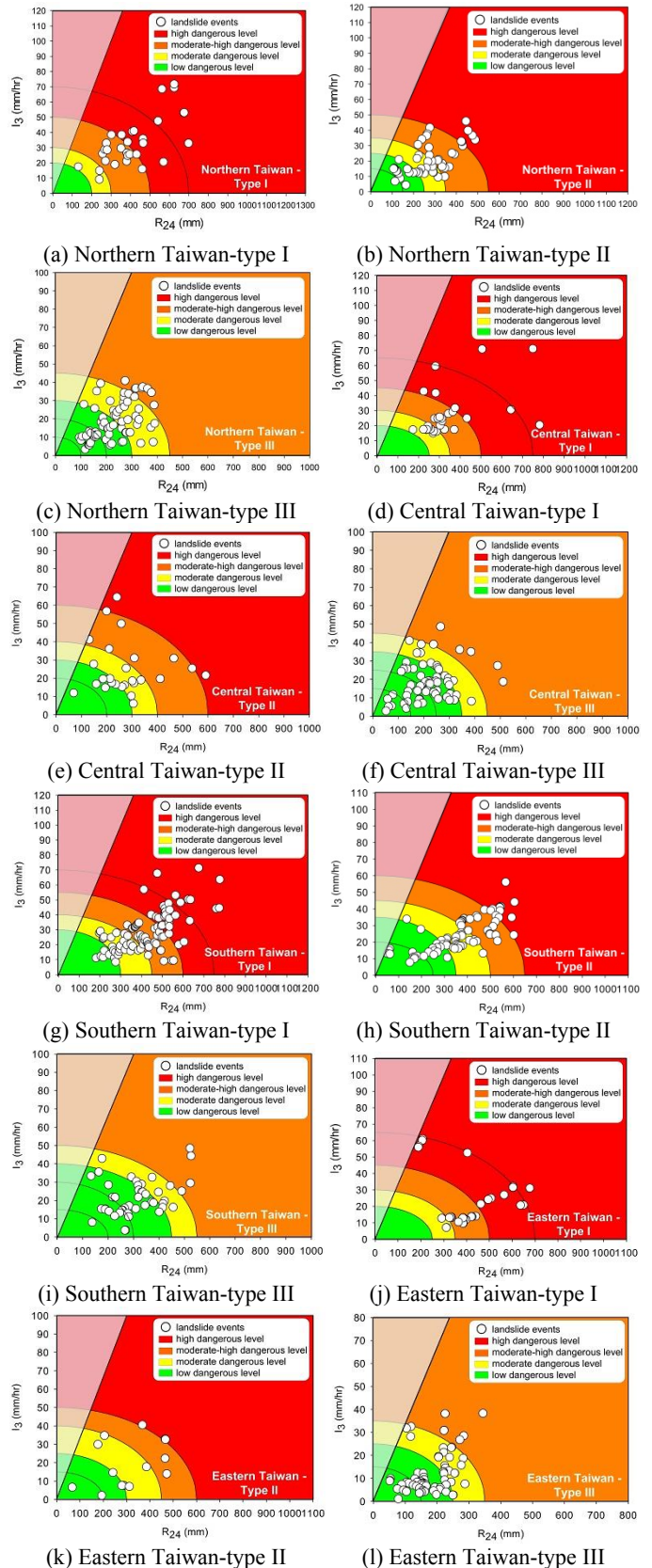


Figure 12 Preliminary rainfall thresholds in Taiwan

Table 6 The validation results of shallow landslide rainfall threshold in northern Taiwan

| Northern Taiwan | H(>=90%) | | M-H(60%) | | M(>=30%) | | L(<30%) | |
|-----------------|-----------------|----------------|-----------------|----------------|-----------------|----------------|-----------------|----------------|
| | R ₂₄ | I ₃ |
| Type I | 700 | 70 | 500 | 50 | 300 | 30 | 200 | 20 |
| Type II | 550 | 50 | 350 | 35 | 250 | 25 | 150 | 15 |
| Type III | 450 | 45 | 300 | 30 | 200 | 20 | 100 | 10 |

Table 7 The validation results of shallow landslide rainfall threshold in central Taiwan

| Central Taiwan | H(>=90%) | | M-H(60%) | | M(>=30%) | | L(<30%) | |
|----------------|-----------------|----------------|-----------------|----------------|-----------------|----------------|-----------------|----------------|
| | R ₂₄ | I ₃ |
| Type I | 750 | 65 | 500 | 45 | 350 | 30 | 250 | 20 |
| Type II | 600 | 60 | 400 | 40 | 300 | 30 | 200 | 20 |
| Type III | 450 | 45 | 350 | 35 | 250 | 25 | 150 | 15 |

Table 8 The validation results of shallow landslide rainfall threshold in southern Taiwan

| Southern Taiwan | H(>=90%) | | M-H(60%) | | M(>=30%) | | L(<30%) | |
|-----------------|-----------------|----------------|-----------------|----------------|-----------------|----------------|-----------------|----------------|
| | R ₂₄ | I ₃ |
| Type I | 750 | 70 | 600 | 55 | 450 | 40 | 300 | 30 |
| Type II | 650 | 60 | 500 | 45 | 350 | 35 | 250 | 20 |
| Type III | 550 | 50 | 450 | 40 | 300 | 30 | 200 | 15 |

Table 9 The validation results of shallow landslide rainfall threshold in eastern Taiwan

| Eastern Taiwan | H(>=90%) | | M-H(60%) | | M(>=30%) | | L(<30%) | |
|----------------|-----------------|----------------|-----------------|----------------|-----------------|----------------|-----------------|----------------|
| | R ₂₄ | I ₃ |
| Type I | 700 | 65 | 500 | 45 | 350 | 30 | 250 | 20 |
| Type II | 600 | 50 | 450 | 40 | 300 | 25 | 200 | 15 |
| Type III | 350 | 35 | 250 | 25 | 150 | 15 | 100 | 10 |

4.3 Landslides Validation and Application

Validation is performed with shallow landslide cases that occurred in Taiwan during Typhoon Matmo, July, 2014 (Figure 13). Ten landslide events that resulted from the aforementioned typhoon event are used to validate the model and to reveal that, if the hazard area or slope unit has no history of landslides, future landslide occurrences during a rainfall event corresponding to an orange to red warning may be accurately predicted landslide potential (snake line) within 2 to 9 hours of the activity. However, for slope units that have a landslide history, new landslide activity may occur during rainfall events that correspond to yellow and green warning levels. This result suggests that the model presented in this study is able to accurately predict the occurrence of landsliding in vulnerable slope units. However, for slope units that have already been disturbed by past landslide activities, as a result of additional environmental factors such as the type and success of vegetative cover treatments, the presence and extent of remediation works, and whether or not the landslide scar is still covered by loose debris, the model is not able to accurately predict due its inability to fully reflect the influence of these factors. When utilizing this model, a yellow warning should be adopted to indicate possible landslide susceptibility in slope units that have a history of landslide disasters. Slope units that have been stable and do not have a history of landslides can be assigned an orange signal as the warning level at which evacuation and other relevant disaster prevention activities are initiated. However, typhoon Matmo did not cause a severe landslide disaster in Taiwan, and more validation results are still needed to ensure that the rainfall thresholds are appropriate.

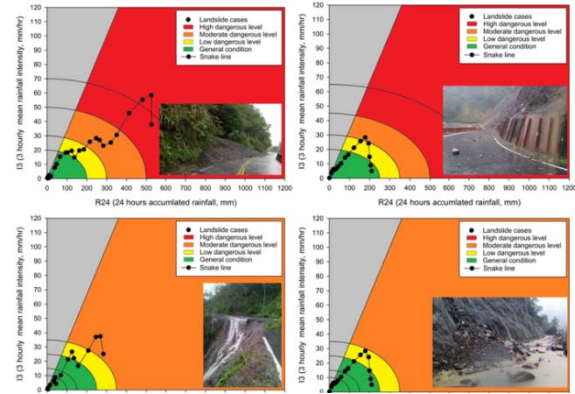


Figure 13 Validations of the rainfall thresholds for shallow landslide

The calibration method and warning system concept employed in this study is shown in Figure 14. Four warning levels are introduced, including green, yellow, orange and red. The warning level for each slope unit is evaluated using measured rainfall data from QPESUMS. From the mode, the snake line associated with the I₃ and R₂₄ values is obtained. If the snake line does not exceed the critical line of 30% landslide occurrence (30% CL), the slope unit is given a green warning level (Condition). This condition indicates that the slope unit is still stable and under typical conditions but the I-R curve associated with the slope unit needs to be monitored. If the I-R curve exceeds the 30% CL curve, a yellow warning signal is achieved (Condition). This level indicates that 30% of past landslide activity occurred at this level and that the landslide potential of the slope unit has already reached a low level of danger. Regarding disaster prevention measures, the evacuation of all residents and resources should be prepared for. Once a yellow warning level has been reached, the model continues to estimate rainfall for the slope unit based on Central Weather Bureau data and to provide rapid estimates of changes in the warning signal. Once the I-R curve exceeds the 60% CL, rainfall conditions have exceeded those that caused 60% of all historic landslides (Condition) and an orange level warning is given; the slope unit has reached a moderate level of danger. At this point, evacuation measures are implemented and the area is closely monitored for further indications of an impending landslide. If the I-R curve exceeds 90% CL, a red level warning is given, which indicates that 90% of all historic landslides associated with the slope unit occurred at or below the current precipitation values. A high danger level is reached and special attention is needed to ensure public safety, particularly for geologically vulnerable areas more susceptible to landslides.

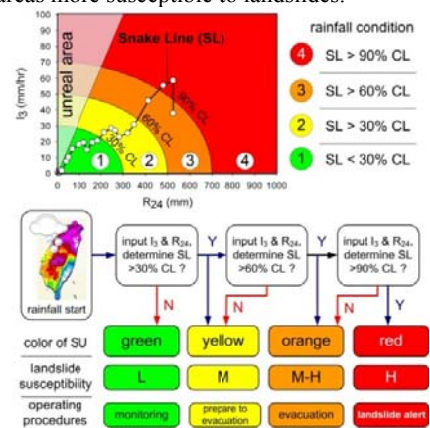


Figure 14 Model calibration and warning system concept for shallow landslide

4.4 Rainfall-induced Landslide Early Warning System

For establishing a real-time warning platform, two important steps are combined into Rainfall-induced Landslide Early Warning System (RiLEWS). Firstly, we divided landslide magnitude into three levels of landslide magnitude according to the landslide ratio for each slope unit (type I, II, and III; Figure 8). Secondly, the real time grid based rainfall data were imported into the slope units in the web-GIS system, to forecast wide-area dynamic landslides susceptibility in real time. This study embeds the Rainfall-induced Landslide Early Warning System within a 3D Web-GIS to immediately announce the landslide hazard map when the external rainfall data is connected (Figure 15). The Web-GIS adopted in the model is an open source system (OPCube™ Server) and more convenient to develop for a specific purpose and publication. The real time grid-based rainfall data (QPESUMS) required in the early landslide warning system was imported from CWB. The landslide hazard susceptibility on each slope unit will be calculated automatically and updated immediately as the accumulated rainfall varies. As the rainfall increases, the system can calculate the snake line (I_3 - R_{24} diagram) immediately and provide the information on the stability of slopes by RiLEWS (Figure 16). As rainfall increases, the signal will turn to orange or red colors indicating that the possibility of failure is higher.

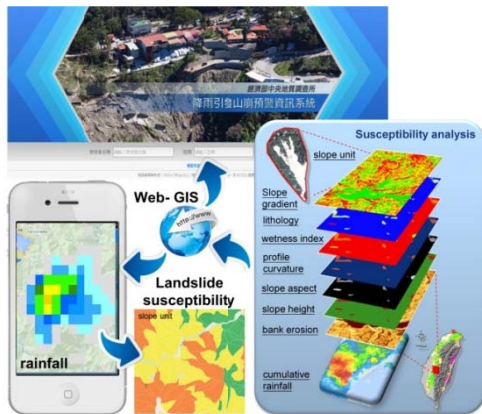


Figure 15 The Rainfall-induced Landslide Early Warning System (RiLEWS)

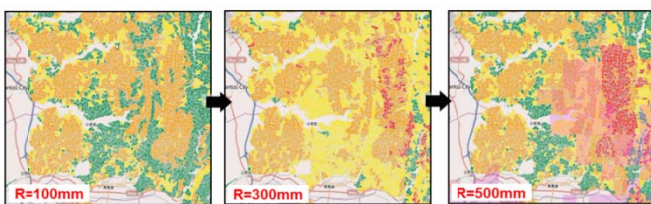


Figure 16 The warning signal of each slope unit according to the input rainfall data variation

The utilization of 3D web-GIS based landslide hazard early warning system has the following benefits: (1) With connection to the real-time rainfall information, the slope unit on the hazard map is updated immediately and announced by the system as the total accumulated rainfall changes. (2) Efficient sharing and exchanging of the landslide hazard warning information are made possible. The local government (ex. village near hillslope) and other related disaster prevention agencies can obtain the updated potential hazard information in time. (3) The unique identification number,

investigation data, remote sensing image, and landslide attributes are all integrated within the slope unit. This provides a convenient interface for user inquiry. (4) System infrastructure satisfies the requirement of emergency response and recovery management, so the responsible agencies can make the necessary decisions in advance according to the potential scenarios.

5. CONCLUSION

This study classifies landslide magnitude as landslide ratio in three categories and establishes the rainfall threshold separately. The combination of magnitude, possibility of occurrence and hazard matrix concept can generate warning signals for a more intuitive execution of evacuation decisions.

Through the analysis of historic landslide data, both 3-hour mean rainfall intensity and 24-hour accumulated rainfall are incorporated into the landslide model developed in this study. As a result, errors associated with past models which failed to incorporate precipitation records or only considered accumulated rainfall are corrected and the accuracy of the model improved. This improved model resulted in the shallow landslide susceptibility model described in this study which had an overall accuracy of 70 % and an AUC value greater than 0.755. Validation results for the non-landslide slope units and the overall accuracy is 73%. The landslide accuracy is 65% and the AUC is 0.737. The result of the analysis supports the conclusion that the model is robust and suitable for wide-area landslide warning systems. Moreover, this study attempts to address landslide disaster severity, a characteristics of landslides not considered in the past, using a hazard level matrix concept. Rainfall thresholds for various levels of severity are developed for the northern, central, southern and eastern zones to ensure improved landslide data for the planning of disaster prevention countermeasures. This study has constructed rainfall thresholds for shallow landslides in the northern, central, southern and eastern zones of Taiwan. Comparisons with recent landslide disasters show that using the snake line to assess landslide susceptibility for both new and enlarging landslides allows early landslide detection and may permit early reaction.

To aid application of these study results, the models and plots summarizing results from the landslide susceptibility and rainfall threshold model will be implanted into the Rainfall-induced Landslide Early Warning System (RiLEWS). By utilizing real-time rainfall records, real-time assessment of the slope failure potential of each slope unit can be obtained to improve the effectiveness of disaster prevention efforts and achieve disaster prevention and reduction goals. Currently, a Web-GIS system has been constructed which is providing data for pre-disaster preparation, during-disaster countermeasures and post-disaster data management. Future landslide triggering rainfall data can be applied to improve the model which in turn will aid landslide predictions for debris flow torrents (source areas), assessments of landslide potential near mountainous highways, and the development of disaster prevention plans for mountainous villages.

6. ACKNOWLEDGEMENTS

The authors would like to thank the Central Geological Survey, MOEA, Taiwan, for supporting this research financially and providing helpful comments on the research (Contract No. 103-5226904000-03-01). The authors also thank Prof. Chyan-Deng Jan of the Department of Hydraulic and Ocean Engineering, National Cheng Kung University, Prof. Kang-Tsung Chang of the Department of Tourism and Hospitality Management, Kainan University, and colleagues in Sinotech Consultants, INC. for their advice and assistance in the study.

7. REFERENCES

- Asselenand, S.V., and Seijmonsbergen, A.C. (2006) "Expert-driven semi-automated geomorphological mapping for a mountainous area using a laser DTM". *Geomorphology*, Vol.78, No.3-4, pp 309-320.
- Ayalew, L., and Yamagishi, H. (2005) "The application of GIS-based logistic regression for landslide susceptibility mapping in the Kakuda-Yahiko Mountains". *Central Japan. Geomorphology*, Vol. 65, No. 1, pp 15-31.
- Bell, F.G. and Maud, R.R. (2000) "Landslides associated with the colluvial soils overlying the Natal Group in the greater Durban region of Natal, South Africa". *Environmental Geology*, Vol. 39, No. 9, pp 1029-1038.
- Brunetti, M.T., Peruccacci, S., Rossi, M., Luciani, S., Valigi, D., and Guzzetti, F. (2010) "Rainfall thresholds for the possible occurrence of landslides in Italy". *Nat. Hazards Earth Syst. Sci.*, Vol. 10, No. 3, pp 447-458.
- Chang, K.T., Chiang, S.H., and Lei, F. (2008) "Analysing the relationship between typhoon triggered landslides and critical rainfall conditions". *Earth Surface Processes and Landforms*, Vol. 33, No. 8, pp 1261-1271.
- Chang, K.T., and Chiang, S.H. (2009) "An integrated model for predicting rainfall-induced landslides". *Geomorphology*, Vol. 105, No. 3-4, pp 366-373.
- Chen, H., Dadson, S., and Chi, Y.G. (2006) "Recent rainfall-induced landslides and debris flow in northern Taiwan". *Geomorphology*, Vol. 77, No. 1, pp 112-125.
- Cheng, C.T., Huang, C.M., Wei, L.W., Lee, C.F., Lee, C.T. (2013) "Landslide Susceptibility Map". ICL Landslide Teaching Tools, International Consortium on Landslides, pp 50-55.
- Corominas, J., and Moya, J. (1999) "Reconstructing recent landslide activity in relation to rainfall in the Llobregat River basin, Eastern Pyrenees, Spain". *Geomorphology*, Vol. 30, pp 79-93.
- Dadson, S. J., Hovius, N., Chen, H., Dade, W. B., Hsieh, M. L., Willett, S.D., Hu, J.C., Hornig, M.J., Chen, M.C., Stark, C.P., Lague, D., and Lin, J.C. (2003) "Links between erosion, runoff variability and seismicity in the Taiwan orogen". *Nature*, Vol. 426, No. 6967, pp 648-651.
- Dilley, M., Chen, R.S., Deichmann, U., Lerner-Lam, A.L., and Arnold, M. (2005) "Natural disaster hotspots: a global risk analysis". ISBN 0-8213-5930-4, World Bank Publications.
- Franklin, J. A., (1975) "Safety and Economy in Tunneling. Proc. 10th Can. Rock Mech. Symp". Queens University, Kingston, Canada, pp 27-53.
- Guzzetti, F., Carrara, A., Cardinali, M., and Reichenbach, P. (1999) "Landslide hazard evaluation: a review of current techniques and their application in a multi-scale study, Central Italy". *Geomorphology*, Vol. 31, No. 1, pp 181-216.
- Guzzetti, F., Peruccacci, S., Rossi, M., and Stark, C.P. (2007) "Rainfall thresholds for the initiation of landslides in central and southern Europe". *Meteorology and atmospheric physics*, Vol. 98, No.3-4, pp 239-267.
- Guzzetti, F., Peruccacci, S., Rossi, M., and Stark, C.P. (2008) "The rainfall intensity-duration control of shallow landslides and debris flows: an update". *Landslides*, Vol. 5, No. 1, pp3-17.
- Hong, Y., Hiura, H., Shino, K., Sassa, K., Suemine, A., Fukuoka, H., and Wang, G. (2005) "The influence of intense rainfall on the activity of large-scale crystalline schist landslides in Shikoku Island, Japan". *Landslides*, Vol. 2, No. 2, pp 97-105.
- Hsu, L.H., Kuo, H.C., and Fovell, R.G. (2013) "On the geographic asymmetry of typhoon translation speed across the mountainous island of Taiwan". *Journal of the Atmospheric Sciences*, Vol. 70, No. 4, pp 1006-1022.
- Kirkby, M.J. (1975) "Hydrograph modelling strategies", in: Peel, R., Chisholm, M., and Haggett, P.: *Process in physical and human geography*, Heinemann, London, pp 69-90.
- Keijsers, J.G.S., Schoorl, J.M., Chang, K.T., Chiang, S.H., Claessens, L., and Veldkamp, A. (2011) "Calibration and resolution effects on model performance for predicting shallow landslide locations in Taiwan". *Geomorphology*, Vol. 133, No. 3-4, pp 168-177.
- Lee, C.T., Huang, C.C, Lee, J.F., Pan, K.L., Lin, M.L., Liao, C.W., Lin, P.S., Lin, Y.S., Chang, C.W. (2004) "Landslide susceptibility analyses based on three different triggering events and result comparison". *Proceeding of International Symposium on Landslide and Debris Flow Hazard Assessment*, Vol. 6-1, pp 6-18.
- Lee, C.T., Huang, C.C., Lee, J.F., Pan, K.L., Lin, M.L., Dong, J.J., (2008^a) "Statistical Approach to Earthquake-Induced Landslide Susceptibility". *Engineering Geology*, 100, No.1-2, pp 43-58.
- Lee, C.T., Huang, C.C., Lee, J.F., Pan, K.L., Lin, M.L., Dong, J.J., (2008^b) "Statistical approach to storm event-induced landslide susceptibility". *Natural Hazard and Earth System Sciences*, Vol. 8, pp 941-960.
- Lee, C.T. (2014) "Statistical Seismic Landslide Hazard Analysis: an Example from Taiwan". *Engineering Geology*, Vol. 182, pp. 201-212.
- Liao, Z., Hong, Y., Wang, J., Fukuoka, H., Sassa, K., Karnawati, D. and Fathani, F. (2010) "Prototyping an experimental early warning system for rainfall-induced landslides in Indonesia using satellite remote sensing and geospatial datasets". *Landslides*, Vol. 7, No. 3, pp 317-324.
- Martelloni, G., Segoni, S., Fanti, R., and Catani, F. (2011) "Rainfall thresholds for the forecasting of landslide occurrence at regional scale". *Landslides*, Vol. 9, No. 4, pp 485-495.
- Martha, T.R., Kerle, N., van Westen, C.J., Jetten, V., and Kumar, K.V. (2012) "Object-oriented analysis of multi-temporal panchromatic images for creation of historical landslide inventories". *ISPRS Journal of Photogrammetry and Remote Sensing*, Vol. 67, pp 105-119.
- Moine, M., Puissant, A., and Malet, J.P. (2009) "Detection of landslides from aerial and satellite images with a semi-automatic method. Application to the Barcelonnette basin (Alpes-de-Hautes-Provence, France)". *Proceedings of the landslide processes conference, Strasbourg, France*, p 63-68.
- Mondini, A.C., Chang, K.T., and Yin, H.Y. (2011) "Combining multiple change detection indices for mapping landslides triggered by typhoons". *Geomorphology*, Vol. 134, No. 3-4, pp 440-451.
- Osanai, N., Shimizu, T., Kuramoto, K., Kojima, S., and Noro, T. (2010) "Japanese early-warning for debris flows and slope failures using rainfall indices with Radial Basis Function Network". *Landslides*, Vol. 7, No. 3, pp 325-338.
- Padilla, C., Onda, Y., Iida, T., Takahashi, S., and Uchida, T. (2014) "Characterization of the groundwater response to rainfall on a hillslope with fractured bedrock by creep deformation and its implication for the generation of deep-seated landslides on Mt. Wanitsuka, Kyushu Island". *Geomorphology*, Vol. 204, pp 444-458.
- Prokesova, R., Medvedová, A., Tábořík, P., and Snopková, Z. (2012) "Towards hydrological triggering mechanisms of large deep-seated landslides". *Landslides*, Vol. 10, No. 3, pp 239-254.
- Razak, K.A., Santangelo, M., Van Westen, C.J., Straatsma, M.W., and de Jong, S. M. (2013) "Generating an optimal DTM from airborne laser scanning data for landslide mapping in a tropical forest environment". *Geomorphology*, Vol. 190, pp 112-125.
- Stumpf, A., and Kerle, N. (2011) "Object-oriented mapping of landslides using Random Forests. *Remote Sensing of Environment*". Vol. 115, No.10, pp2564-2577.
- Turkington, T., Ettema, J., van Westen, C.J., and Breinl, K. (2014) "Empirical atmospheric thresholds for debris flows and flash

- floods in the Southern French Alps". *Natural Hazards and Earth System Sciences*, Vol. 2, pp 757-798.
- Vessia, G., Parise, M., Brunetti, M.T., Peruccacci, S., Rossi, M., Vennari, C., and Guzzetti, F. (2014) "Automated reconstruction of rainfall events responsible for shallow landslides". *Natural Hazards and Earth System Sciences*, Vol. 2, pp 2869-2890.
- Wilson, J.P. and Gallant, J.C. (2000) "Terrain analysis", John Wiley & Sons, Inc., pp479.
- Wu, C.H., Chen, S.C., and Chou, H.T. (2011) "Geomorphologic characteristics of catastrophic landslides during typhoon Morakot in the Kaoping Watershed, Taiwan". *Engineering Geology*, Vol. 123, No. 1, pp 13-21.
- Xie, M., Esaki, T., and Zhou, G. (2004) "GIS-based probabilistic mapping of landslide hazard using a three-dimensional deterministic model". *Natural Hazards*, Vol. 33, No.2, pp 265-282.
- Zêzere, J.L., Trigo, R.M., and Trigo, I.F. (2005) "Shallow and deep landslides induced by rainfall in the Lisbon region (Portugal): assessment of relationships with the North Atlantic Oscillation". *Natural Hazards and Earth System Sciences*, Vol. 5, pp 331-344.
- Zhou, W., Tang, C., Van Asch, T.W., and Zhou, C. (2014) "Rainfall-triggering response patterns of post-seismic debris flows in the Wenchuan earthquake area". *Natural Hazards*, Vol. 70, No. 2, pp 1417-1435.